Sparse Photoacoustic Microscopy Reconstruction Based on Matrix Nuclear Norm Minimization

Ying Fu[1], Naizhang Feng[1], Yahui Shi[1], Ting Liu[2], and Mingjian Sun[1(✉)]

[1] Department of Control Science and Engineering,
Harbin Institute of Technology at Weihai, Weihai 264209, China
`fu_ying_hit@163.com, fengnz@yeah.net,`
`295182727@qq.com, sunmingjian@hit.edu.cn`
[2] Department of Measurement and Control Technology and Instrumentation,
Dalian Maritime University, Dalian 116026, China
`liuting15348@126.com`

Abstract. As a high-resolution deep tissue imaging technology, photoacoustic microscopy (PAM) is attracting extensive attention in biomedical studies. PAM has trouble in achieving real-time imaging with the long data acquisition time caused by point-to-point sample mode. In this paper, we propose a sparse photoacoustic microscopy reconstruction method based on matrix nuclear norm minimization. We use random sparse sampling instead of traditional full sampling and regard the sparse PAM reconstruction problem as a nuclear norm minimization problem, which is efficiently solved under alternating direction method of multiplier (ADMM) framework. Results from PAM experiments indicate the proposed method could work well in fast imaging. The proposed method is also be expected to promote the achievement of PAM real-time imaging.

Keywords: Sparse photoacoustic microscopy reconstruction
Real-time imaging · Matrix completion · Nuclear norm minimization

1 Introduction

Photoacoustic microscopy (PAM) has been considered as an effective tool for high-resolution deep tissue imaging in biomedical studies, such as imaging of tumor microenvironments, brain functions and gene activities [1–5]. In PAM, the lateral resolution is defined by the overlap of both optical excitation and ultrasound detection's foci, which are focused on the same spot, while the axis resolution is defined by the acoustic time of fight. According to the sizes of optical excitation and ultrasound detection's foci, PAM is divided into optical-resolution PAM (OR-PAM) and acoustic-resolution PAM (AR-PAM) [6]. In conventional PAM, the measured data X is detected by point-to-point mechanical scanning of ultrasound and optical components on the target surface to obtain high resolution of deep tissue. This sampling of PAM is one kind of oversampling (Fig. 1(a)). More sampling points are necessary for higher

resolution. However, it leads to consuming more sampling time, larger data size and more requirements for system hardware. The most common way to enhance the resolution is to improve the performances of objective and ultrasound transducer, which will increase the system cost. For example, to increase optical numerical aperture (NA) of objective can improve resolution for OR-PAM, but it also means that the penetration depth will be decreased at the same time and the optical scanning devices should have higher performance indexes [4, 5]. Thus, it's significant for PAM to improve the scanning speed with no influence to resolution under limited experiment condition.
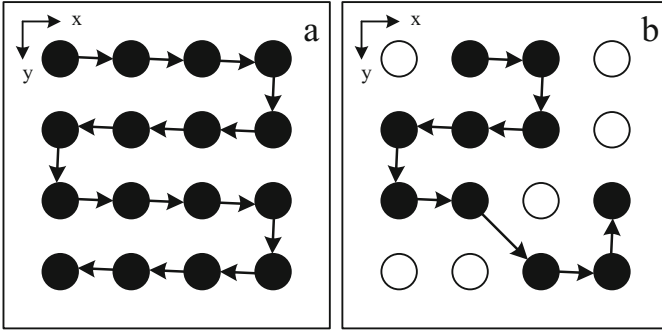
Fig. 1. (a) Scanning path of the traditional full-sampling mode; (b) scanning path of the sparse sampling mode

In many studies, it's shown that most medical images are sparse by themselves or proper transformation including photoacoustic images [7, 8]. The sparsity of photoacoustic imaging has been proven and fully utilized to obtain highest-resolution photoacoustic image by the least amount of sampling data [9, 10]. In particular, the application of compressive sensing (CS) technology in photoacoustic tomography (PAT) has achieved remarkable success and received excellent experiment results [11], but CS application in PAM is rare. What's more, the conventional sampling of PAM is one kind of oversampling. We can achieve fast data acquisition by decreasing measurement numbers with sparse sampling method, whose scanning path is shown in Fig. 1(b). In sparse sampling mode, the random sampling mask A can be generated if sampling rate (SR) k and sampling point numbers m, n in direction of x, y respectively are known. Here assume $A \in \mathbb{R}^{m \times n}$ as a 0, 1 matrix, where 1 means the point's data needs to be collected while 0 means not. According to the sampling mask A, computer can plan shortest scanning path to achieve sparse scanning and minimize sampling time. Therefore, the sparse PAM measured data $b \in \mathbb{R}^p$ is defined as

$$b_l = X_{i,j} \text{ if } A_{i,j} = 1, \ 1 \le i \le m, \ 1 \le j \le n, \ 1 \le l \le p, \ p < m \times n, \quad (1)$$

where $X \in \mathbb{R}^{m \times n}$ is final PAM image what we want to recover i.e. the measured data of conventional PAM and $A \in \mathbb{R}^{m \times n}$ is sparse sampling mask.

In this paper, we propose a method to solve a sparse photoacoustic microscopy reconstruction problem, which is to acquire the real images from fast-scanning data, i.e. recover PAM image $X \in \mathbb{R}^{m \times n}$ from compressive measured data $b \in \mathbb{R}^p$.

2 Method

According to sparse PAM reconstruction problem, we attempt to recover complete matrix $X \in \mathbb{R}^{m \times n}$ from measured matrix $b \in \mathbb{R}^p$ which can be approximately regarded as a part of X. It can be described as a matrix recovery problem, also known as a matrix completion problem. Recht et al. proved that most matrices $X \in \mathbb{R}^{m \times n}$ which has low-rank property can be recovered from $b \in \mathbb{R}^p$ if the entries of A are suitably random e.g., i.i.d. Gaussian [12, 15]. Fortunately, as a result that the low-rank property of photoacoustic imaging has been verified in recent studies [13], sparse PAM recon-struction problem can be transformed to the completion problem of low-rank matrix, which takes low-rank property for a constraint. Thus, sparse photoacoustic microscopy reconstruction problem is defined as:

$$
\begin{aligned}
&\min \ \mathrm{rank}(X) \\
&\text{s.t.} \ \mathcal{A}(X) = b \text{'}
\end{aligned}
\tag{2}
$$

where $X \in \mathbb{R}^{m \times n}$ is the decision variable, $\mathcal{A} \colon \mathbb{R}^{m \times n} \to \mathbb{R}^p$ is the sampling map, and vector b is measured.

Due to the problem (1) is a NP-hard problem in general, we can replace rank (X) with the nuclear norm of X, which is the tightest convex relaxation of rank(X) [14, 15]. Approximating nuclear norm to the rank function, the problem (1) can be trans-formed into the form as below [16]:

$$
\begin{aligned}
&\min \ \|X\|_* \\
&\text{s.t.} \ \mathcal{A}(J) = b, \ X = J \text{'}
\end{aligned}
\tag{3}
$$

where $\|X\|_* := \sum_{i=1}^{r} \sigma_i(X)$ is the nuclear norm of X which has r positive singular values of $\sigma_1 \geq \sigma_2 \geq \ldots \geq \sigma_r > 0$.

To solve the problem conveniently, the problem (3) is transformed to the form of corresponding augmented Lagrangian function

$$
\begin{aligned}
L_\mu(X, J, x, j) =\ & \|X\|_* - \langle x, X - J \rangle - \frac{\mu_1}{2} \|X - J\|_F^2 - \langle j, \mathcal{A}(J) - b \rangle \\
& + \frac{\mu_2}{2} \|\mathcal{A}(J) - b\|_2^2,
\end{aligned}
\tag{4}
$$

where $x \in \mathbb{R}^{m \times n}$, $j \in \mathbb{R}^p$ is the Lagrangian multiplier, and $\mu_1 > 0$ and $\mu_2 > 0$ are the penalty parameters for the linear constraint.

The solution can be obtained by solving the problem (3) under ADMM [17], described as follows:

$$X_{k+1} = \arg\min_X \|X\|_* + \frac{\mu_1}{2}\left\|X - (J_k + \frac{1}{\mu_1}x_k)\right\|_F^2, \tag{5}$$

$$J_{k+1} = \arg\min_J - \langle x_k, X_{k+1} - J\rangle + \frac{\mu_1}{2}\|X_{k+1} - J\|_F^2 - \langle j_k, \mathcal{A}(J) - b\rangle \\ + \frac{\mu_2}{2}\|\mathcal{A}(J) - b\|_2^2, \tag{6}$$

$$x_{k+1} = x_k - \gamma_1(X_{k+1} - J_{k+1}), \tag{7}$$

$$j_{k+1} = j_k - \gamma_2(\mathcal{A}(J_{k+1}) - b), \tag{8}$$

where γ_1 and γ_2 are the penalty parameters for the linear constraint.

Assume $X \in \mathbb{R}^{m\times n}$ and the SVD of X is $X = U\mathrm{Diag}(\sigma)V^T$, $U \in \mathbb{R}^{m\times r}$, $\sigma \in \mathbb{R}_+^r$, $V \in \mathbb{R}^{n\times r}$. For any $v > 0$, the matrix shrinkage operator $\mathcal{S}_v(\cdot)$ is defined as [15]

$$\mathcal{S}_v(X) := U\mathrm{Diag}(\bar\sigma)V^T, \text{ with } \bar\sigma := \begin{cases} \sigma - v, & \sigma - v > 0 \\ 0, & \text{o.w.} \end{cases}, \tag{9}$$

Obviously, the closed solution of X-subproblem (4) can be described as

$$J_{k+1} = \mathcal{S}_{\frac{1}{\mu_1}}(J_k + \frac{1}{\mu_1}x_k)J_k \text{ and } x_k, \tag{10}$$

On the other hand, nothing the right value of J-subproblem (5) as $f(J)$, a unique solution of it can obtained by taking partial derivatives with respect to J, i.e., $\partial f(J)/\partial J = 0$, described as

$$(\mu_1 I + \mu_2(\mathcal{A}^*\mathcal{A}))J = \mu_1 X_{k+1} - x_k - \mathcal{A}^*(\mu_2 b + j_k), \tag{11}$$

where I is an identity matrix, and $\mathcal{A}^*$ is the adjoint of $\mathcal{A}$. The linear operator equation can be solved easily by the conjugate gradient method.

Based on the discussion above, we summarize the algorithm for sparse photoacoustic microscopy reconstruction problem based on matrix nuclear norm minimization via ADMM in Table 1, where *maxiter* is maximum number of iterations, *tol* is termination criterion for iteration.

3   Experimental Results

In this section, experiment results on several PAM images for solving sparse PAM reconstruction problem are reported, which show the efficiency of the proposed method (Algorithm 1). In order to evaluate the performances of proposed method qualitatively and quantitatively, four performance indexes are utilized. They are: peak signal-to-noise

Table 1. Reconstruction algorithm based on matrix nuclear norm minimization via ADMM.

Reconstruction algorithm based on matrix nuclear norm minimization via ADMM
Input: b, μ_1, μ_2, γ_1, γ_2, $maxiter$, tol, $k=0$, $X_0 = \mathbf{0}$, $J_0 = \mathbf{0}$, $x_k = \mathbf{0}$, $j_k = \mathbf{0}$
for k=0,1,…,$maxiter$
1. Compute X_{k+1} via (9) with fixed J_k and x_k;
2. Compute J_{k+1} via (10) with fixed X_{k+1}, x_k and j_k;
3. Update x_k and j_k with fixed J_{k+1} and X_{k+1};
4. If $\left\| X_{k+1} - X_k \right\| \leq tol$, stop and return X_{k+1};
5. End if;
6. End for;
Output: $X = X_{k+1}$

ratio (PSNR), structural similarity (SSIM) index, relative error (Rerr) and mean square error (MSE), respectively.

$$PSNR = 10 * \log_{10} \frac{mn}{\sum\limits_{i=1}^{m} \sum\limits_{j=1}^{n} (X_{ij} - Y_{ij})^2}, \tag{12}$$

$$SSIM(X, Y) = \frac{(2\mu_X \mu_Y + C_1)(\sigma_{XY} + C_2)}{(\mu_X^2 + \mu_Y^2 + C_1)(\sigma_X^2 + \sigma_Y^2 + C_2)}, \tag{13}$$

$$\mathrm{Re}rr = \frac{\|X^K - X\|_2}{\|X\|_2}, \tag{14}$$

$$MSE = \frac{\sum\limits_{i=1}^{m} \sum\limits_{j=1}^{n} (X_{ij} - Y_{ij})^2}{mn}, \tag{15}$$

where X is the approximate optimal solution of problem (3), i.e. restored image, and Y is the reference image. μ_X, μ_Y are respectively mean of X and Y, σ_X and σ_Y are respectively variance of X and Y and σ_{XY} is covariance of image X and Y. C_1 and C_2 are constants to prevent denominator from being zero [18].

In our experiments, we obtain two groups of PAM images by full-sampling and random-sampling PAM system. The first group is PAM images of mouse brain (resolution: 211×211), whose sample rates (SR) are respectively 1.0, 0.6, 0.5, 0.4, 0.3, 0.2, 0.1; another group is of mouse ear (resolution: 954×954), whose sample rates are same to the first group. Figures 2(a)–(d) and Figs. 3(a)–(d) show two groups of typical experimental results from the method described above. The values of Rerr, MSE, PSNR and SSIM obtained in different sampling rate by the proposed method are

summarized in Table 2. As can be seen, when the sampling rate is 0.4, the recovered images of both two groups have already having relatively good resolution. The PSNRs between the recovered images and the reference images are over 40 dB and the SSIMs are 1, which indicate the proposed method has a great effectiveness. It is also worth noting that less sampling rate means less sampling time.
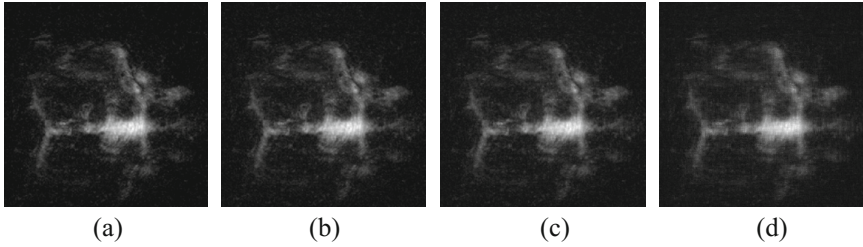
Fig. 2. Results from mouse brain images. (a) Full sampling image. (b)–(d) Recovered images by our method which sampling rates are 0.6, 0.4, 0.2, respectively.
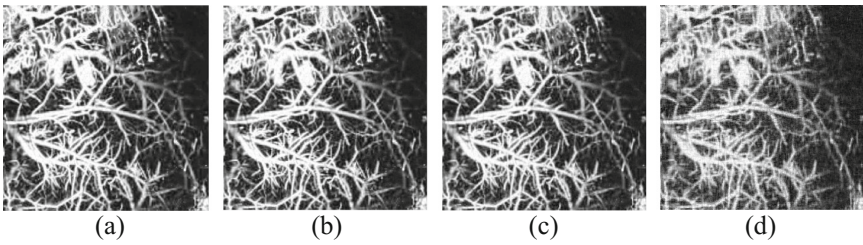
Fig. 3. Results from mouse ear images. (a) Full sampling image. (b)–(d) Recovered images by our method which sampling rates are 0.6, 0.4, 0.2, respectively.

Table 2. The results in different sampling rate by the proposed method

	SR	0.6	0.5	0.4	0.3	0.2	0.1
Group 1	Rerr	0.0379	0.0608	0.0927	0.1340	0.1930	0.3060
	MSE	0.0047	0.0075	0.0114	0.0165	0.0237	0.0376
	PSNR	47.3873	45.3329	43.5004	41.3871	40.3105	38.3176
	SSIM	1.0000	1.0000	1.0000	1.0000	1.0000	0.9999
Group 2	Rerr	0.0379	0.0608	0.0927	0.1340	0.1930	0.3060
	MSE	0.0112	0.0150	0.0263	0.0493	0.0944	0.1761
	PSNR	43.5818	42.3096	40.0256	37.1342	34.3135	31.6086
	SSIM	1.0000	1.0000	1.0000	0.9998	0.9993	0.9970

4 Conclusion

In conclusion, we present a sparse photoacoustic microscopy reconstruction method to recover complete PAM images from parts of images. It aims to reduce data acquisition time and reconstruct the real images from fast-scanning data from fast-scanning data. An efficient matrix completion algorithm has been proposed to solve the associated optimization problem. The results from PAM experiments demonstrate the proposed method could work well in fast imaging, so we expect that the study can be applied in actual operation and provide a way for the achievement of PAM real-time imaging. For further study, the case that the image is not sparse at all will be considered.

References

1. Wang, L.V., Hu, S.: Photoacoustic tomography: in vivo imaging from organelles to organs. Science **335**(6075), 1458 (2012)
2. Yao, J., Wang, L.V.: Photoacoustic Microscopy. Laser Photonics Rev. **7**(5), 758–778 (2013)
3. Zhang, H.F., Maslov, K., Stoica, G., Wang, L.V.: Functional photoacoustic microscopy for high-resolution and noninvasive in vivo imaging. Nat. Biotechnol. **24**, 848–851 (2006)
4. Zhang, C., Maslov, K., Hu, S., et al.: Reflection-mode submicron-resolution in vivo photoacoustic microscopy. J. Biomed. Opt. **17**(2), 020501 (2012)
5. Wu, Z.H., Sun, M.J., Wang, Q., et al.: Photoacoustic microscopy image resolution enhancement via directional total variation regularization. Chin. Opt. Lett. **12**, 104–108 (2014)
6. Zhou, Y., Wang, L.V.: Translational photoacoustic microscopy. In: Olivo, M., Dinish, U.S. (eds.) Frontiers in Biophotonics for Translational Medicine. POSP, vol. 3, pp. 47–73. Springer, Singapore (2016). https://doi.org/10.1007/978-981-287-627-0_2
7. Provost, J., Lesage, F.: The application of compressed sensing for photo-acoustic tomography. IEEE Trans. Med. Imaging **28**(4), 585–594 (2009)
8. Liang, D., Zhang, H.F., Ying, L.: Compressed-sensing photoacoustic imaging based on random optical illumination. Int. J. Funct. Inf. Personal. Med. **2**(4), 394–406 (2009)
9. Guo, Z., Li, C., Song, L., et al.: Compressed sensing in photoacoustic tomography in vivo. J. Biomed. Opt. **15**(2), 021311 (2010)
10. Sun, M., Feng, N., Shen, Y., et al.: Photoacoustic imaging method based on arc-direction compressed sensing and multi-angle observation. Opt. Express **19**(16), 14801–14806 (2011)
11. Wu, Z.H., Sun, M.J., Wang, Q., et al.: Compressive sampling photoacoustic tomography based on edge expander codes and TV regularization. Chin. Opt. Lett. **12**(10), 41–45 (2014)
12. Recht, B., Fazel, M., Parrilo, P.A.: Guaranteed minimum-rank solutions of linear matrix equations via nuclear norm minimization. SIAM Rev. **52**(3), 471–501 (2007)
13. Liu, T., Sun, M., Feng, N., et al.: Sparse photoacoustic microscopy based on low-rank matrix approximation. Chin. Opt. Lett. **9**, 62–66 (2016)
14. Fazel, M.: Matrix rank minimization with applications. Ph.D. thesis, Stanford University (2002)

15. Ma, S., Goldfarb, D., Chen, L.: Fixed point and Bregman iterative methods for matrix rank minimization. Math. Program. **128**(1), 321–353 (2011)
16. Jin, Z., Wan, Z., Jiao, Y., Lu, X.: An alternating direction method with continuation for nonconvex low rank minimization. J. Sci. Comput. **66**(2), 849–869 (2016)
17. He, B.S., Liao, L.Z., Han, D.R., et al.: A new inexact alternating directions method for monotone variational inequalities. Math. Program. **92**(1), 103–118 (2002)
18. Sreelekha, G., Koparde, P.G.: Perceptual video coder incorporating wavelet based Intra frame coder. In: International Conference on Computer and Communication Technology, p. 188193. IEEE Press, Allahabad (2010)